Turk J Phys
28 (2004) , 31 – 39.

AMPS-1D Modeling of a-Si:H n^+-i-n^+ Structure: the Validity of Space Charge Limited Current Analysis

A. ERAY[1*], **G. NOBILE**[2]
[1]*Hacettepe University, Department of Physics Engineering,*
06532 Beytepe, Ankara-TURKEY
[2]*ENEA Research Center, Loc. Granatello, I-80055, Portici (NA)-ITALY*
e-mail: feray@hacettepe.edu.tr

Received 28.07.2003

Abstract

In this paper, the AMPS-1D (Analysis of Microelectronic and photonic structure) simulation program is used to understand the origin of the differences observed in Space Charge Limited Current (SCLC) analysis in thin and thick a-Si:H n^+-i- n^+ structure. For that purpose, the problem of applicability of SCLC measurements to n^+-i-n^+ a-Si:H samples are investigated by using both the thin (0.3 μm) and thick (3 μm) samples. The simulation results show that activation energy in thick samples is larger than in thinner samples, which are an agreement with the experimental results. It is emphasized that this method is highly useful for good quality a-Si:H samples, even if it is a thin sample, and den Boer analysis gives correct information about the density of states. This information comes from the states in the upper limited part of the gap, as exhibited by the lower activation energy of thin samples.

Key Words: AMPS-1D, Hydrogenated amorphous silicon, n^+-i-n^+ structure, SCLC, activation energy.

1. Introduction

Since computer models are an excellent tool for studying transport mechanism and as a method that can lead one to better device design, amorphous silicon alloy device modeling has been receiving a great deal of attention in the last 15 years. In the literature, there are several computer programs for modeling amorphous silicon solar cells. Examples are: the model of Hack and Shur [1], the program AMPS developed at Penn State University [2], the ASPIN program from Ljubljana University [3] and the ASA package developed at Delft University of Technology [4]. All these computer programs are limited to one-dimensional (1-D) modeling.

Device modeling involves the numerical solution of a set of equations, which form a mathematical model for device operation, and the models that describe material properties and device operation processes. The usefulness of the simulation results strongly depends on the reliability of the input parameters that are required by the internal numerical models. By using simulation programs, it is possible to examine the influence of model parameters, which cannot be determined experimentally. As the model parameters can be set independently from one another, the results of the changes in device configuration can be determined much faster.

*Corresponding author

In this paper, we use the one-dimensional device simulation program AMPS-1D (Analysis of Microelectronic and photonic structure) developed at Pennsylvania State University, to understand the origin of the differences observed in Space Charge Limited Current (SCLC) analysis in thin and thick a-Si:H n^+- i- n^+ structures. SCLC is a classic and a well-known method to determine the density of states in the mobility gap of amorphous hydrogenated silicon and has been applied to a large variety of materials [5–10].

For SCLC measurements, charge injection is needed and therefore the measurements are mostly made on metal-semiconductor-metal sandwich structures with both contacts being ohmic for electrons (or holes), in n^+-i-n^+ (or p^+-i-p^+) devices. To improve the injection of electrons (holes) into the intrinsic layer, heavily doped contact layers are used. In n^+-i- n^+ structures, the electrons are injected from one of the n^+ layers into the intrinsic region, while the other n^+ layer blocks the injection of holes. Since the injected electrons are trapped on empty gap states close to the Fermi energy, an increase in the voltage drop across the i-type layer increases the number of the trapped electrons and shifts E_F toward the conduction band, leading to population of the empty gap states towards the conduction band edge. At low applied voltages, the excess space charge and consequently the Fermi level shift is negligible. When the injected charge is not great enough to appreciably increase the electron concentration above its equilibrium value, the I-V characteristics shows a nearly ohmic behavior, and the conductivity is approximately equal to that of the bulk [5–9]. At high electric fields, when the injection is large enough to significantly displace the quasi Fermi Level from its equilibrium position, the current starts to rise super linearly. This is the SCLC regime. Since the magnitude of the current and the shape of the I-V characteristics depend on the density of states just above the equilibrium Fermi Level, the space charge limited part of the curve can be used to determine the density of states.

In the literature, there are several methods for the analyzing of J-V characteristics that allow obtaining energy profile of gap states [5–10]. The validity of the SCLC relies on a few assumptions, and one of them is that the n^+/i interfaces have no influence on the electron transport in the i-layer. In the literature, it is reported that this is valid only if the thickness of the i-layer is large enough, and for the thin films SCLC does not gives the correct DOS information [5, 7-8]. In our previous paper [9–11], we employed den Boer analysis to obtain the defect density of states distribution in the only limited part of the band gap of the sample; and we emphasized that, in a good quality sample, even for a thin sample, den Boer analysis gives correct information about the density of states . In that model, depending on the value of the activation energy, the starting point of the quasi Fermi level shifts will change. So, the DOS values obtained in the thin samples having much lower activation energy values reflects the information in different regions of the gap which resides in the upper part of gap.

In this paper, AMPS–1D simulation program is used to search the validity of SCLC in thin n^+-i-n^+ a-Si:H samples and to provide extra information that is not available by experiment (such as the band profiles, the electric field, the concentration of free carriers, trapped carriers and space charges as a function of position). This information will help us to understand the processes that take place in thin devices and to establish a link between the properties of the layers considered in the model and the device characteristics. Details of the simulation results including the investigations of the electric field profile, of the concentration of free carriers, and of the space charges, all as a function of position for thin and thick samples at various applied bias voltages, is presented here.

2. AMPS-1D Analysis

The one-dimensional device simulation program AMPS-1D solves the Poisson equation and the electron and hole continuity equations by using the method of finite differences and the Newton-Raphson technique [12].

The numerical simulation requires a model of the density of states (DOS) in the sample. For the density of localized states in the mobility gap, it has been assumed that there are both acceptor like states (in the upper half of the gap) and donor like states (in the lower half of the gap). Both of these acceptor and donor

like states consist of exponential band tail states and Gaussian midgap states (dangling bonds). The density of localized states in the gap of undoped a-Si:H is assumed to comprise the exponential band-tail states and Gaussian midgap states, and the density of a doped a-Si:H is assumed to comprise the band-tail states, the dangling-band states, and the donor states. The valence band and the conduction band tail states have an exponential distribution in energy and is given as follows:

$$[N(E)]_{vt} = N(E_v)\, exp\left[\frac{E_v - E}{E_D}\right], \quad [N(E)]_{ct} = N(E_c)\, exp\left[\frac{E - E_c}{E_A}\right], \tag{1}$$

where $N(E_v)$ and $N(E_c)$ are the densities of tail states at the band edge energies E_v and E_c, respectively; and E_A and E_D are the characteristics slopes of the conduction band tail states and the valence band tail states, respectively.

The midgap states are described by the Gaussian distribution for acceptor-like states, donor-like states and also donor states via

$$[N(E)]_{db} = \frac{N_{db}}{\sigma_{db}\sqrt{2\pi}} \cdot exp\left[-\frac{(E - E_{db})^2}{2\sigma_{db}^2}\right], \tag{2}$$

where E_{db}, N_{db} and σ_{db} are the energy position, density and the variance of these the dangling bonds, respectively. Here, N_{db} represents the density of states per volume per energy. AMPS is set-up to ask for the total number of states per volume in a Gaussian. The energies for the donor-like and acceptor-like states are measured positively up from the valence band and positively down from the conduction band, respectively [12].

Since the states can exchange carriers with the conduction and valence bands, capture cross sections for each states must be specified for electron and hole capture. Therefore, AMPS requires definition of the capture cross sections for neutral and charged states, for both free holes and electrons.

AMPS 1-D solves the set of transport equations subject to very general boundary conditions at the front metal-n^+ layer contact ($x = 0$) and at the back metal-n^+ layer contact ($x = L$). These boundary conditions are defined at the front and back contact in terms of electron barrier heights and surface recombination speeds [12]. In the model, in the thermodynamic equilibrium, at the front ($x = 0$) and back ($x = L$) surface, the barrier heights for electrons is specified as

$$\phi_{b0} = [E_c - E_f]_{x=0} \quad \text{and} \quad \phi_{bL} = [E_c - E_f]_{x=L} \tag{3}$$

Here, E_c is the conduction band edge and E_f is the Fermi-level position in thermo dynamic equilibrium.

In this study, the n-layer doping is selected very carefully, which gives an activation energy for this n-layer material of $E_{act} = 0.2$ eV (see Table). This value agrees with the range of conductivity activation energy reported for the n-layer material [9] and corresponds to a bulk value of $E_c - E_F = 0.2$ eV. To avoid the influence of the band bending at the front and back contact, ϕ_{b0} and ϕ_{bL} values were chosen to position the Fermi Level in the contact at $x = 0$ and $x =$ L at the same energy at which it would be positioned in the n-layer by doping.

Since the model contains so many parameters, most of the model parameters can be fixed to measured values for device quality a-Si:H, leaving only a few gap-state parameters free. It is well known that all parameters cannot be determined from experiments. Therefore, it can be difficult to obtain realistic values for these parameters. In this modeling study, the input parameters are obtained from experimental results published data in the literature. The set of parameters used in this study to simulate a typical hydrogenated amorphous silicon n^+-i-n^+ structure are given in Table. Donor-like and acceptor-like tail states are represented with characteristic slopes of 50 meV and 30 meV, respectively. The densities of states at the bottom

of the conduction bands and the top of the valence bands are assumed to be the same. The charged capture cross-section σ_c (involving a charged defect) was fixed at 5×10^{-15} cm^2, while the neutral cross-section σ_n was assumed to be smaller by a factor of 100. The width of the Gaussian distributions was set at 0.1 eV. Since $E_{act} = 0.2$ eV in the bulk of the n-layer material used in this study, n-layer Fermi energy was set 0.2 eV below the conduction band edge, and had the same band edges as intrinsic layer.

Table. Parameters for a-Si:H used in this simulation.

	i-layer	n-layer
Layer thickness (μm)	0.3–3	0.03
Mobility gap (eV)	1.75	1.75
Effective density of states N_c, N_v (cm^{-3})	2.5×10^{20}	2.5×10^{20}
Electron mobility (cm^2 V^{-1}s^{-1})	10	1
Hole mobility (cm^2 V^{-1}s^{-1})	10	1
Total DOS in donor-like Gaussian (cm^{-3})	5×10^{15}	6×10^{17}
Total DOS in acceptor-like Gaussian (cm^{-3})	5×10^{15}	3×10^{17}
Standard deviation in donor-like Gaussian (eV)	0.1	0.07
Standard deviation in acceptor-like Gaussian (eV)	0.1	0.15
Position of donor-like Gaussian (eV) (from Ec)	0.9	0.1
Position of acceptor-like Gaussian (eV) (from Ev)	1.2	1.25
Energy slope donor-like band tail (meV)	50	50
Energy slope acceptor-like band tail (meV)	30	30

3. Simulation Results and Discussions

Figure 1 shows schematically the energy band diagram of the n$^+$-i-n$^+$ structure at zero bias and at a positive bias V obtained by computer simulation. E_c and E_v are the energetic positions of the conduction and valence band edges and E_F is equilibrium Fermi Level. In this figure, the simulation result of the position dependent conduction band and valence band for a n$^+$-i-n$^+$ structure are plotted using the parameters in Table. This figure shows that the Fermi level E_F at the n$^+$-i and i-n$^+$ interfaces lies $\sim$0.2 eV below the electron mobility edge E_c, where as in the bulk of structure it approximates to the value of 0.75 eV, for thick samples. When a bias is applied to a n$^+$-i-n$^+$ structure, electrons are injected from the back contact at $x = L$ (on the right hand side of Figure 1) and collected by the forward-biased front metal electrode at $x = 0$. Since the metal n$^+$ layer contact at $x = 0$ blocks the injection of holes, one type of carrier current is established in this structure.

As a first step of the simulation, thick samples ($L = 3$ μm) are chosen and the SCLC theory is reviewed. Then the results are compared with those of the thin samples ($L = 0.3$ μm).

In Figures 2a–2d, the potential distribution, the electric field, free electron and space-charge density profiles are plotted as a function of position for n$^+$-i-n$^+$ structure, with an intrinsic layer thickness of $L =$ 3 μm and both n$^+$ layers of $L_n = 0.03$ μm. In analyzing the spatial variation of the transport parameters, various applied biases have been selected in order to investigate both ohmic region and space charge region. Without going to details, it should be mentioned that when the forward bias exceeds the value of 2 V, the conduction mechanism would be space charge limited for thick samples [5–8].

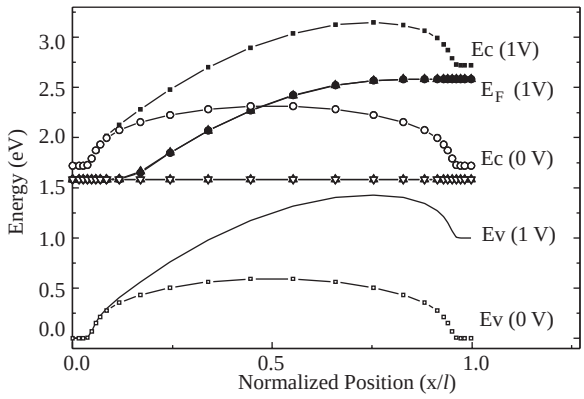

Figure 1. Schematic band diagram of n^+-i-n^+ structure at zero bias and at a positive bias, eV. The horizontal axis is chosen as normalized position where x is the position and L is the thickness.

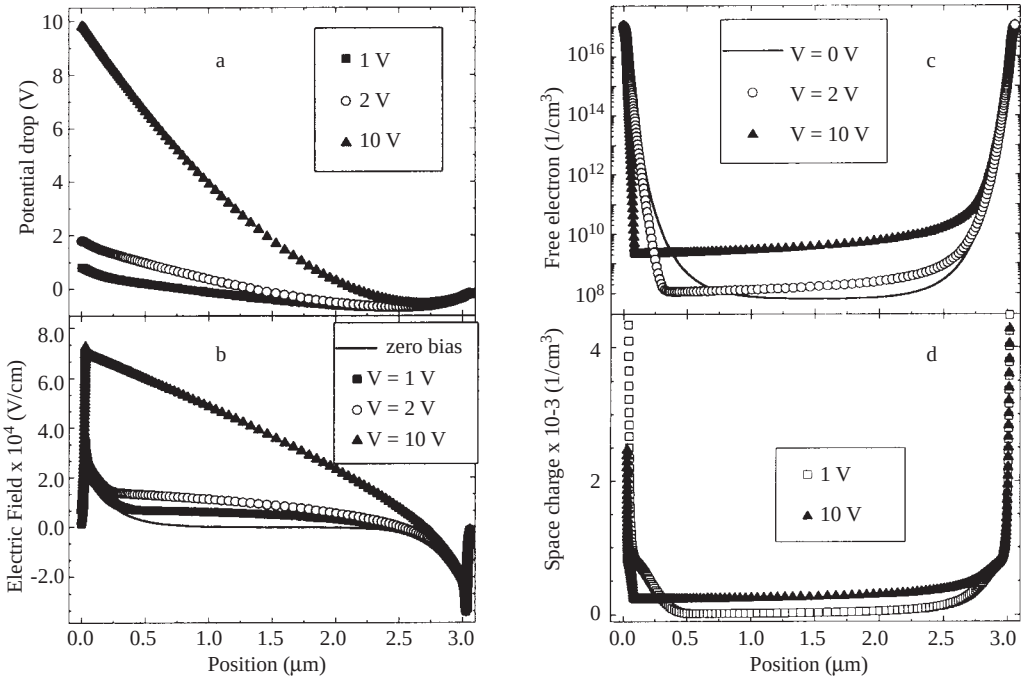

Figure 2. Profiles of (a) potential drop, (b) electric field, (c) free electron concentration, (d) space-charge density of n^+-i- n^+ structure with an intrinsic layer thickness of 3 μm at various applied bias.

Figure 2a–2b show the distribution of the potential drop, $V(x)$, and also the electric field profile under different applied biases. Potential drop is small in doped layers when compared to that over the undoped intrinsic layer. As seen in Figure 1 and Figure 2a, the conduction and valence band edges are parallel to $V(x)$. As explained in the introduction, when the applied bias increases, the current increases and becomes space charge limited. In good agreement with this general observation, i.e. as an indicator of the transition from ohmic region to space charge region, the voltage profiles change from linear to quadratic function of position; whereas the field profiles change from uniform to linear function of position, with applied bias. As mentioned above and seen in Figure 1, the electrons are injected from the right contact, which is the injection contact. Injected electrons are trapped in localized gap states located in the intrinsic layer and n-layers, and they build up a virtual cathode potential barrier near the i/n interface, as shown in Figure 2a. The position

of the maximum barrier is where the electric field changes sign and this point is the *virtual cathode*. At zero bias, this virtual cathode is at the middle of the device and moves towards the zero-potential electrode as the external bias is increased, Figure 2b. As a result of potential profile, which is quadratic function of position, the maximum of the electric field has a value of $2V/L$ and its position is close to the collecting contact (at $x = 0$).

The free electron concentration profile is plotted in Figure 2c. It can be seen that the electron concentration in both n^+-layers is almost 10^{17} cm^3, and decays very rapidly at the n^+-i interfaces, reaching the bulk level within 0.5 μm from the injection contact. There is also an increase in the free electron concentration, with increasing the applied bias, as expected from theory. But the injected electrons, i.e. the electrons that are injected from the right contact into the intrinsic region, cause a small concentration gradient within the bulk of the intrinsic layer, although it can be seen that the electron concentration is relatively uniform over most of the device thickness.

Concerning the negative space charge profile, as seen in Figure 2d, it is similar in shape to the free electron concentration profile. The extra negative space charge accumulates at the injecting contact and also over the most of the undoped layer and with increasing bias the equilibrium accumulated space charge becomes depleted close to the collecting contact.

Figure 3 shows the electric field profile for the thin samples, having different defect density for the intrinsic layer, with an intrinsic layer thickness of L = 0.3 μm and both n^+-layers of $\underline{L}_n = 0.03$ μm. These thin samples are named as *good* quality or *poor* quality samples, depending on the DOS in the i-layer. For the *poor* quality thin samples, the DOS in the i-layer has been selected as 5×10^{16} states /cm^3, whereas the value of 5×10^{15} states/cm^3 for *good* quality samples. Figure 3 is similar in shape to Figure 2c. It is seen that there is a difference between the applied bias for the good and bad quality samples. This can be explained as follows: when the injected charge is great enough to appreciably increase the electron concentration above its equilibrium value, this regime is space charge limited. As a result, for the samples having much higher defect density in intrinsic layer, higher applied biases is needed to reach above their equilibrium DOS values and hence the space charge region.

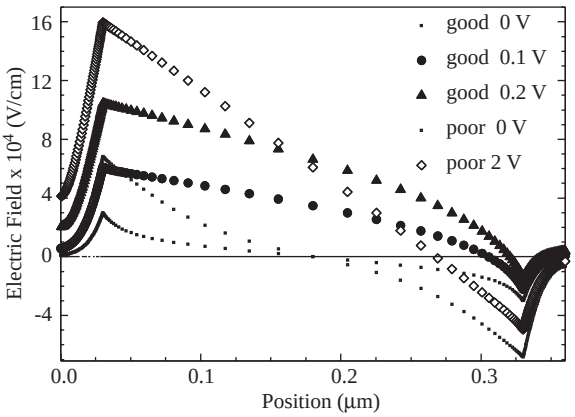

Figure 3. Electric field profiles for two thin samples, having different defect density for the intrinsic layer, with an intrinsic layer thickness of $L = 0.3$ μm. Details are given in the text.

The electric field in the sample is an important aspect of the transport behavior in devices. Under the usual assumption of SCLC, there is assumed to be an infinite supply of free electrons and zero electric field at the injection contact [6, 8]. However, as can be seen easily from Figure 2c and Figure 3, the zero electric field position, which is the virtual cathode, is situated in the middle of the device, and it gradually shifts towards the injecting contact with increasing bias, in both thick and thin samples. From the results above, it can be deduced that is no observed significant difference between the thick and thin samples.

In order to clarify the cause of the incorrect DOS information for thin samples in the literature [5-8], we examined the profiles of the conduction band edge E_c with respect to the thermo dynamic equilibrium Fermi level E_{fo} as a function of the position, for the samples having different i-layer thickness and defect density. Results are given in Figure 4 and Figure 5.

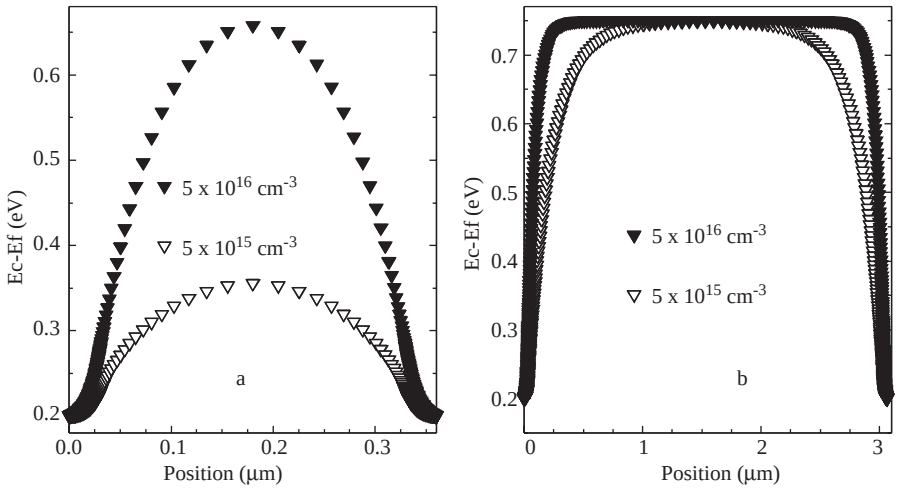

Figure 4. The energy profiles ($E_c - E_f$) for two n^+-i-n^+ samples having *good* (5×10^{15}states/cm^3) and *poor* (5×10^{16} states/cm^3) quality intrinsic layer (a) with a thickness of 0.3 μm, (b) with a thickness of 3 μm.

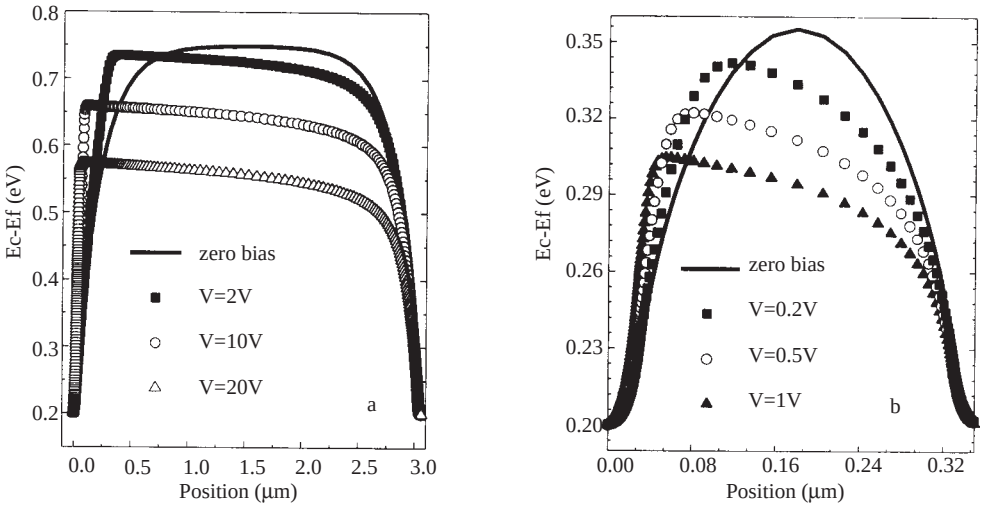

Figure 5. The applied bias dependence of the activation energy, both the *good* quality (a) thick and (b) thin samples.

Figure 4a shows the profiles of the conduction bang edge E_c with respect to the thermo dynamic equilibrium Fermi level E_{fo} as a function of the position for two n^+-i-n^+ samples, having different defect density of states in the intrinsic layers, each with a 0.3 μm thick undoped i-layer and 30 nm thick n^+ layers. In the same manner, Figure 4b represents the similar profiles of $E_c - E_f$, for the two thicker samples, each with a 3 μm thick undoped i-layer and 30 nm thick n^+ layers. The profiles correspond to samples in thermodynamic equilibrium. Since the activation energy of the samples is determined to represent the distance between the conduction band edge and the Fermi Level for the bulk i-layer, for the thick samples, the activation energy is larger than the corresponding shorter device, as seen in Figure 4. These results are in agreement with

numerical calculations in the literature; the high E_a values are obtained only for thickness greater than 4 μm [13–17]. It is clear from Figure 4a that the activation energy of 0.75–0.8 eV, for undoped a-Si:H is never obtained at any point of the thin samples. In the thin samples of *good* quality having low DOS ($5{\cdot}10^{15}$ cm^3), the depletion width extends across the i-layer of structure and this gives the low values of activation energy E_a. For the *poor* quality samples having $5{\cdot}10^{16}$ states/cm^{-3} , due to the large DOS in the i-layer, the depletion width is reduced giving an abrupt n^+/i interface and the activation energy is larger than for the case of the device with a *good* quality i-layer. When the i-layer DOS of the thicker sample is increased to $5{\cdot}10^{16}$states/cm^3, a plateau in the potential profile is observed towards the center of the device. This corresponds to a complete collapse of the electric field in the region. Charge trapping in the large number of gap states results in high electric fields close to the n/i interfaces and a consequent collapse of the bulk electric field [15].

The activation energy of the n^+-i-n^+ structure reflects the effects of the n^+ contacts (band bending) and low density of states above mid-gap, which places E_F close to the conduction band. Without such bending, the activation energy would be determined by E_F in the bulk a-Si:H, which in high quality materials is near mid-gap (in the range 0.75–0.8 eV) [14–15]. As reported in our previous paper, the activation energies, obtained experimentally from the ohmic region of the J-V curves in n^+-i- n^+ samples, are 0.30–0.32 eV [9]. This experimental value is in a good agreement with our simulation results, as seen in Figure 4a. As we emphasized in our previous paper [9], in SCLC analysis, depending on the value of activation energy, the starting point of the quasi Fermi level shifts will change. So, the DOS values obtained in the thin samples having much lower activation energy values reflects the information in different regions of the gap which resides in the upper part of gap.

Figure 5a and 5b are plotted to investigate the applied bias dependence of the activation energy, both the *good* quality thick and thin samples, respectively. As expected from the theory, with increasing the applied bias, the quasi Fermi level shifts to the conduction band edge, giving the lower values of $E_C - E_F$, for both samples. From these Figures, it is interesting to mention that, in the space charge region, after the first rapid increase at the injecting contact, the quasi-Fermi energy increases again slowly within the bulk of the undoped layer to its maximum value (the position of the *virtual anode*) and decreases at the collection contact. When the applied bias is increased, the position of the maximum, the virtual anode, shifts to the collection contact.

4. Conclusion

In this study, we performed simulations with an examination of the effects of varying thickness, and midgap density of state levels in an attempt to determine what materials and conditions are necessary for the SCLC measurements to yield a correct DOS.

We conclude that the DOS is not thickness dependent in good quality samples. The obtained low activation energies in thin device quality n^+-i-n^+ samples and the high activation energies for the thick ones are the representative of this main conclusion. SCLC analysis gives correct information about the density of states in the limited part of the band gap of the sample, for good quality samples, even if thin. This information refers to the density of states near the conduction band tail, which resides in the upper limited part of the gap, due to the lower activation energy exhibited by thin samples. Using a series of good quality samples of different thickness, the investigation range of the DOS can be extended into various portions of the gap.

The results of our study are important, for they open a window on the question of whether SCLC method is valid for thinner n^+-i-n^+ samples.

Acknowledgements

The author would like to thank Prof. S. Fonash at Pennsylvania State University for providing the computer program used in the simulations.

References

[1] M. Hack, M. Shur, R., *J. of Appl. Phy.,* **58,** (1985), 997.

[2] P.J. McElheny, J. Arch, H.S. Lin, S.J. Fonash, *J. of Appl. Phy.,* **64 (3)**, (1988), 1254.

[3] F. Smole, J. Furlan, *J. of Appl. Phy.,* **72**, (1992), 5964.

[4] M. Zeman, J.A.Willemen, L.L.A.Vosteen, G. Tao, J.W. Metselaar, *Solar Energy Materials & Solar Cells,* **46,** (1997), 81.

[5] W. den Boer, *J. Phys. (Paris)*, **42 (NC4),** (1981), 451.

[6] S. Nespurek, J. Sworakowski, *J. of Appl. Phy.*, **51(4),** (1980), 2098.

[7] K.D. Mackenzie, P.G. LeComber, W.E. Spear, *Phil. Mag.*, **46,** (1982), 377.

[8] R.L. Weisfield, *J. of Appl. Phy.,* **54,** (1983), 6401.

[9] A. Eray, G. Nobile, *Solar Energy Materials & Solar Cells,* **76 (4)**, (2003), 521

[10] A. Eray, G. Nobile, Proceedings of the NATO ASI on Photovoltaic and Photoactive Materials-Properties, Technology and Applications, Ed. By J. M. Marshall, D. Dimova-Malinovska, (Kluwer Academic Publishers, London, 2001), p. 253

[11] A. Eray, G. Nobile, *Journal of Material Scince-Materials in Electronics,* **14,** (2003), 735.

[12] S.V. FonAsh, J. Arch, J. Cuiffi, J. Hou, W. Howland, P. McElheny, A. Moquin, M. Rogossky, F. Rubinelli, T. Tran and H. Zhu, A manual for AMPS-1D for Windows 95/NT; A one-dimensional device simulation program for the analysis of microelectronic and photonic structures, (Pennsylvania State University, 1997).

[13] V. Cech, *Solid State Electronics,* **41**, (1997), 81.

[14] R.M. Dawson, J.H. Smith, C.R. Wronski, *MRS Symp. Proc.*, **192,** (1990), 145.

[15] P. Chatterjee, R. Vanderhaghen, B. Equer, *MRS Symp. Proc.*, **420,** (1996), 233.

[16] J. H. Smith, S.J.Fonash, *J. of Appl. Phy.* **72,** (1992), 5305.

[17] C. Molenbroek, C.H.M. Van Der Werf, K.Feenstra, F. Rubinelli, E.I. Schropp, *MRS Symp. Proc.* **467,** (1997), 717.